J Mater Sci (2011) 46:2851–2859
DOI 10.1007/s10853-010-5159-z

# The stability of $BaFe_{12}O_{19}$ nanoparticles in polar solvents

**Darja Lisjak · Simona Ovtar · Miha Drofenik**

Received: 3 September 2010 / Accepted: 4 December 2010 / Published online: 16 December 2010


**Abstract** We have studied suspensions of hard-magnetic $BaFe_{12}O_{19}$ particles in water, ethanol and 1-butanol. The surfaces of these particles were previously modified with the surfactant dodecylbenzylsulphonic acid. The stabilities of the suspensions were estimated from their saturation concentrations and zeta potentials. We found that the 1-butanol suspensions were more stable than the ethanol-based suspensions and much more stable than the water-based suspensions. We analyzed the suspensions and the dispersed particles using gravimetry, conductometry and transmission electron microscopy, measured their zeta potentials, and calculated the interparticle-attraction interaction energies due to the van der Waals and magnetic dipole–dipole forces. The magnitudes of the attraction energies varied significantly with the particles' sizes and the separation distances between the particles, and we found that the contribution of the van der Waals attraction energy can be neglected with respect to the magnetic dipole–dipole attraction. The observed differences in the stability of the suspensions were explained on the basis of the calculated electrostatic and steric repulsion energies. Electrosteric stabilization was possible in the 1-butanol and the ethanol for particles with radii and thicknesses up to 15 nm, while a too small electrostatic repulsion and the absence of steric repulsion in the water resulted in rapid agglomeration.

D. Lisjak (✉) · S. Ovtar · M. Drofenik
Department for Materials Synthesis, Jožef Stefan Institute, 1000 Ljubljana, Slovenia
e-mail: darja.lisjak@ijs.si

M. Drofenik
Faculty of Chemistry and Chemical Engineering, University of Maribor, 2000 Maribor, Slovenia

## Introduction

Ba ferrite, $BaFe_{12}O_{19}$, is a well-known magnetic material that is suitable for a variety of applications, like electric motors, magnetic recording, microwave and millimetre-wave devices and absorbers. Depending on the application, Ba ferrite is used in the form of bulk, powder, films or composites. Composite materials can have properties that match, or even exceed, those of the constituent phases [1–4]. Magnetic particles are also used for biomedical and technical applications in the form of suspensions, like ferrofluids and magneto-rheological fluids [5–8].

The main problem during the preparation of homogeneous magnetic composites and magnetic suspensions is how to overcome the magnetic attraction between the particles and, consequently, to prevent their agglomeration. In general, particles tend to agglomerate due to the attraction by the van der Waals forces when they approach at distances of a few nanometres [9]. Magnetic particles are additionally attracted by the magnetic dipole–dipole forces. Stabile suspensions can be prepared when a high enough electrostatic and/or steric repulsion is provided between the particles by the application of surfactants or polymers [5, 6, 9–14].

Other existing solutions to the agglomeration problem were applied to soft-magnetic particles, which can be directly synthesized in a carrier liquid or in a polymer matrix at low temperatures [15, 16]. The particles' surfaces are coated with a non-magnetic layer, which prevents any magnetic attraction between the particles. Such surface-modified particles can then be subsequently incorporated into various matrices. Minimum temperatures of 500 °C are required for the crystallization of Ba ferrite [17, 18], and these temperatures are too high for any synthesis in liquids. An alternative solution is to replace the organic polymers with Si-based polymers (i.e., tetraetyhletoksi

silane = TEOS) [19–21]. Here, ferrite precursors crystallize into ferrites coated with $SiO_2$, which crystallizes from the TEOS during annealing at 600–1100 °C [19, 21]. However, this synthesis is only appropriate for spinel ferrites. In the case of Ba ferrite precursors, Ba silicates crystallize together with Fe oxides instead of only Ba ferrite and $SiO_2$ [18].

It seems to be a very challenging task to synthesize Ba ferrite composites or composite particles directly. Therefore, it would be of great advantage if the as-synthesized Ba ferrite particles could be dispersed in a solvent in which each individual particle could later be coated with the nonmagnetic layer. The aim of this work was to study the stabilization of single-domain Ba ferrite particles in polar solvents.

## Theory and calculation

Ba ferrite particles suspended in a solvent are attracted by the van der Waals and magnetic dipole–dipole forces. The van der Waals attraction energy ($E_{vdw}$) depends on the separation distance between the particles ($l$) and on the electrodynamic interactions between the species at the particle's surfaces and the solvent molecules included in Hamaker constant ($A$). The magnetic dipole–dipole interaction energy ($E_m$) depends on the magnetic properties of the particles and on the separation distance between the particles. The Ba ferrite particles in our study were plate-like and single domain. Such a single-domain magnetic particle is fully saturated and so it aligns easily in the direction of the magnetic field. The magnetic axis of a Ba ferrite particle has the same direction as its crystallographic $c$-axis, i.e., perpendicular to the large surface of the particles. Consequently, single-domain Ba ferrite particles will align with their large planes together and form columnar agglomerates. Since our aim was to estimate the largest possible attractive interaction energies between the two particles, the magnetic repulsion contribution was neglected in our calculations. The described geometry was considered in our calculation of the attraction energy between the Ba ferrite particles using Eqs. 1 and 2 [13, 22], derived from generally known equations [2, 9, 23, 24].

$$E_{vdw} = -\frac{A}{12\pi}\left(\frac{1}{l^2} + \frac{2}{(l+2r\sqrt{\pi})^2} - \frac{2}{(l+r\sqrt{\pi})^2}\right) rl\sqrt{\pi} \tag{1}$$

$$E_m = -\frac{\mu_0}{4\pi}\frac{(M_s D\pi r^2 h)^2}{(l+h)^3} \tag{2}$$

Here, $r$ is the radius of a particle and $D$ is its density, $h$ is the thickness of a particle, $l$ is the separation distance between the particles, $\mu_0 = 4\pi \times 10^{-7}$ J/Am$^2$ is the permeability of a vacuum and $M_s$ is the saturation magnetization of Ba ferrite. In the calculations we considered crude Ba ferrite particles with no surfactant layer. The Hamaker constant ($A$) for the ferrite/water system was considered to be $4.5 \times 10^{-20}$ J, as previously in [22], and the Hamaker constants for the Ba ferrite/1-butanol and Ba ferrite/ethanol systems were estimated as in [25, 26] and were approximately $A \sim 5.3 \times 10^{-20}$ J for the 1-butanol and $A \sim 2.0 \times 10^{-20}$ J for the ethanol.

The repulsive interaction potential due to the electrostatic and steric forces arising from the surfactant layer was also considered. The electrostatic interaction potential ($E_R$) between two particles can be calculated with Eq. 3 [9].

$$E_R = F\frac{\varepsilon_r\varepsilon_0}{4}\left[2\psi_1\psi_2 \ln\left(\frac{1+e^{-\kappa l}}{1-e^{-\kappa l}}\right) + \left(\psi_1^2+\psi_2^2\right)\ln\left(1-e^{-2\kappa l}\right)\right] \tag{3}$$

where $1/\kappa = \sqrt{\frac{\varepsilon_0\varepsilon_r kT}{e_0^2\sum_i n_i Z_i^2}}$

$$E_R = \frac{\varepsilon_r\varepsilon_0\varsigma^2 r^2}{2h}\left[\ln\left(\frac{1+e^{-\kappa l}}{1-e^{-\kappa l}}\right) + \ln\left(1-e^{-2\kappa l}\right)\right] \tag{4}$$

Here, $F$ is a geometry factor, $\psi_{1,2}$ is the surface potential and can be approximated with the measured zeta potential ($\zeta$) [9, 11], $\kappa$ is the reciprocal Debye–Hückel parameter, $\varepsilon_0 = 8.854 \times 10^{-12}$ As/Vm is the permittivity constant of a vacuum and $\varepsilon_r$ is the relative permittivity of a solvent, $n_i$ is the number density of the ion $i$ in the medium and $Z_i$ is the charge of the ion $i$, and $e_0 = 1.6022 \times 10^{-19}$ As is the elementary electron charge and $k = 1.38 \times 10^{-23}$ J/K is the Boltzman constant. Considering the plate-like geometry, Eq. 4 can be derived from Eq. 3.

The evaluation of the steric interaction is even more complex than that of the electrostatic [10, 12, 14]. First, the steric interaction only acts at relatively short separations: up to double the thickness of the surfactant layer ($l \leq 2t$). Second, the interaction mechanism between the surfactant's chains and its strength depends on the density of the surfactant molecules/chains and their interaction with the solvent. The stabilizing layer around the particles usually consists of the surfactant and the solvent molecules, and the surfactant concentration has to be determined together with the so-called Flory–Huggins parameter ($\chi$) for each system: a surfactant is soluble in a solvent if $\chi \leq 0.5$ [12]. The third, and the most difficult parameter to determine, is the interaction volume of the surfactant layer between the two approaching particles. This is because not all the surfactant chains repel when two particles approach at a small enough distance. Some of the surfactant chains may partially interpenetrate from the stabilizing layer of one particle into another, and some molecules may be desorbed or

even attracted by special functional groups. In addition, a certain volume fraction of the solvent is squeezed out and, consequently, the surfactant concentration increases. A simplified calculation of the steric energy is given in Eq. 5 [27], where a good solvent was assumed ($\chi = 0$) and the fact that the used surfactant was a much shorter molecule than the long polymer chains was neglected.

$$E_s \approx \frac{kT}{a}\left[\ln\left(\frac{1}{1-\phi}\right) - \phi\right]\left\{\frac{\pi\delta^2}{12}\left[6\left(\frac{h}{2}+t\right) - \delta\right]\right\} \quad (5)$$

Here, $a$ is a monomer length (in this study the largest fragment of the DBSa molecule was considered = 0.24 nm), $\phi$ is the volume fraction of the surfactant in a surface layer with a thickness $t$ (=2 × 2 nm, in our study) and $\delta$ is the thickness of the overlapping surfactant layer between the two particles, where $\delta = 0$ for $l \geq 2t$ and $\delta = 2t - l$ for $l < 2t$.

In general, the strong enough repulsion results in an energy maximum that prevents the agglomeration of the particles if it is large enough (≥5 kT). In the absence of the energy maximum, rapid agglomeration occurs and its rate can be expressed by Eq. 6, where $k_0$ is the rate constant and $\eta$ is the viscosity of the medium [11]. However, in the presence of an energy maximum ($E_{max}$) the rate of agglomeration ($k$) becomes slower and can be expressed with Eq. 7 [11].

$$k_0 = \frac{8kT}{6\eta} \quad (6)$$

$$k = \frac{k_0}{W}, \text{ where } W = \frac{1}{2}e^{E_{max}/kT} \quad (7)$$

## Experimental procedure

### Powders

In this study we used commercial Ba ferrite particles (Aldrich, Steinheim, Germany) with a stated average diameter of 60 nm. This commercial powder was selected because it is easily available to other researchers and because a similar powder morphology and particle-size distribution is obtained with the majority of soft-chemical synthesis methods [28–30]. Observations with a transmission electron microscope (TEM, Jeol 2100, Tokyo, Japan) revealed that the particles were platelets with a broad particle-size distribution (Fig. 1a), and the particles' sizes were determined from several TEM images (as an example, see Fig. 2a in "Stability of the suspensions" section). Although the statistics of the determined thicknesses were poorer than those of the radii, due to the preferential alignment of the anisotropic particles, we managed to get reliable values by inspecting a sufficient number of TEM images. We were able to distinguish roughly five fractions (see table inserted in Fig. 1a).

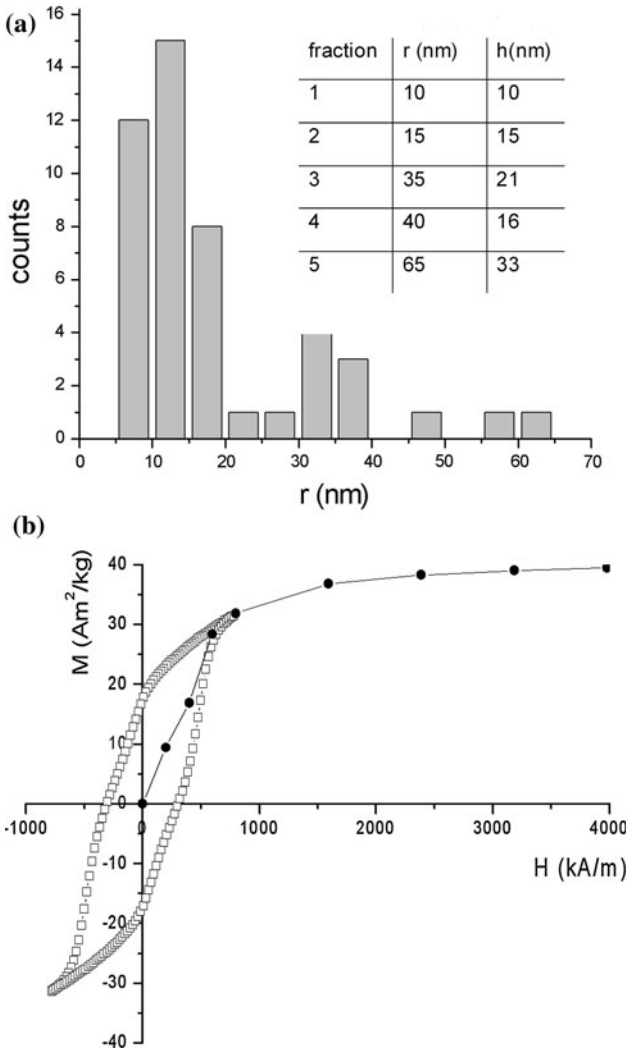


**Fig. 1** The particle-size distribution of the studied Ba ferrite powder (**a**) and its magnetization curve (**b**) measured with VSM (*squares*) and with SQUID (*circles*), where $r$ denotes the radius and $h$ denotes the thickness

The magnetic properties of the Ba ferrite powder were measured with a vibrating-sample magnetometer (VSM, Lake Shore 7312, Westerville, OH, USA). The particles exhibited typical ferrimagnetic behaviour (Fig. 1b), with a high coercivity of 306 kA/m, which is typical for hard magnets, and a remanent magnetization of 17 Am$^2$/kg. The magnetization at the maximum applied field of 800 kA/m was 31 Am$^2$/kg. However, this field of 800 kA/m was not enough to saturate the particles due to their high magnetocrystalline anisotropy (1353 kA/m) [31]. Therefore, an additional measurement was carried out with a Quantum Design SQUID magnetometer (MPMS XL-5, San Diego, CA, USA) that had a maximum magnetic field of 1980 kA/m. The saturation magnetization of the Ba ferrite powder measured at 1980 kA/m was $M_s$ = 39 Am$^2$/kg (Fig. 1b). This is an average value for the whole powder; it was not

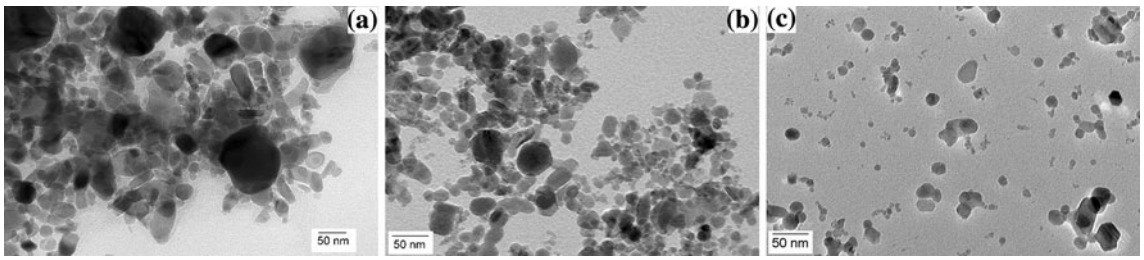


**Fig. 2** TEM images of the studied Ba ferrite particles from the 1-day-old water (**a**) and the 1-butanol (**b**) suspensions and from the 6-day-old 1-butanol suspension (**c**)

**Table 1** Basic materials properties used in the calculations: the abbreviations are the same as used in the main document

| Property | Ba ferrite | 1-Butanol | Ethanol | Water |
|---|---|---|---|---|
| $M_s$ ($Am^2/kg$) | 20 (fractions 1–2) | | | |
| | 39 (fractions 3–5) | | | |
| $\rho$ ($kg/m^3$) | 5300 | 800 | 789 | 1000 |
| $\eta$ (mPa s) | | 2.99 | 1.2 | 1.0 |
| $n$ | 2 | 1.3993 | 1.361 | 1.3330 |
| $\varepsilon$ | | 17.84 | 24.6 | 78.5 |
| $\zeta$ (mV) | | +52 | +39 | −23 (pH = 8) |
| | | | | −40 (pH ≥ 10) |
| $n_i$ ($m^{-3}$) | | $1.7 \times 10^{26}$ | $1.4 \times 10^{26}$ | $7.2 \times 10^{28}$ |
| $1/\kappa$ (nm) | | 12.15 | 15.74 | 1.23 |
| $\phi$ | | 0.18 | 0.20 | |

possible to measure directly the $M_s$ of particles with a specific size. Therefore, we estimated the $M_s$ value (Table 1) for the two smallest size fractions, 1 and 2, based on the literature data and considering the surface effect on the $M_s$ value of the nanoparticles [32, 33] to be $M_s \sim 20$ $Am^2/kg$, while the measured value $M_s \sim 39$ $Am^2/kg$ was considered for the larger size fractions, 3–5.

### Suspensions

The Ba ferrite suspensions in water were prepared with dodecylbenzenesulphonic acid (DBSa; Alfa Aesar, Karlsruhe, Germany). The Ba ferrite powder was milled with the DBSa in water (mass ratio Ba ferrite:DBSa: $H_2O$:$NH_3$ = 1:2:40:0.08) for 2 h in a planetary mill. $NH_3$ was used to adjust the pH to a value of 11. After milling, the slurry was diluted 20× with water and then ultrasonicated (VCX500 Ultrasonic Processor, Sonics & Materials, Newtown, CT, USA) with a power of 250 W for 3 s. A slightly different procedure was used for the preparation of the Ba ferrite suspensions in ethanol and in 1-butanol. The Ba ferrite powder, water and DBSa (mass ratio Ba ferrite:DBSa:$H_2O$ = 10:1:300) were mixed together. The pH value of the suspension was fixed with 1-M $HNO_3$ at 1.5. The suspension was then stirred at the boiling point of water for 2.5 h. Next, the suspension was cooled down and washed with water and acetone to remove any surplus DBSa. After that the powder was dried at 60 °C and re-dispersed in ethanol or 1-butanol with pulsed ultrasound (300 W/puls and 5 min).

The stability of the Ba ferrite particles was determined with zeta potential measurements (Zeta PALS Zeta Potential Analyzer, Brookhaven Instruments Corporation, Holtsville, NY, USA), taking into account the solvents' dielectric constants, viscosities and refractive indices (see Table 1). The pH during the measurements of the water suspensions was varied between 2 and 11 with the HCl or NaOH solutions (0.1 or 1 M). The zeta potentials of the saturated suspensions in ethanol and 1-butanol were measured with single-point measurements. The concentrations of the suspensions were analyzed on the first and sixth day after the suspensions were prepared in order to obtain the saturation concentration of the stabile suspensions by weighing the suspension before and after the heat treatment at 420 °C. The total concentration of the DBSa was also determined in this way. The concentration of the DBSa, dissolved in a solvent, was determined with a measurement of the conductivity (Conductometer Knick—Portamess, cell constant 0.475) by using a standard addition method. The concentration of the DBSa on the particles' surfaces was calculated from the difference between the total and the dissolved fractions of the DBSa. The dried particles from the suspensions were deposited on a Cu grid and observed with a Jeol 2100 TEM.

## Experimental results and discussion

### Stability of the suspensions

The stability of the suspensions was examined with gravimetric tests after various sedimentation times. The concentrations of Ba ferrite particles in the 1-day-old suspension prepared with the initial powder concentration of 1 mass% (see "Suspensions" section) were 0.042 vol.% in 1-butanol, 0.031 vol.% in ethanol and 0.02 vol.% in water.

The concentration of the Ba ferrite particles decreased after 6 days to 0.021 vol.% in 1-butanol and to 0.019 vol.% in ethanol, while the water suspensions sedimented completely in 6 days.

TEM images (Fig. 2) show the dispersed particles and some remaining agglomerates. The fraction of dispersed particles in the 1-butanol is higher than in the water. This is consistent with the superior stability of the 1-butanol suspensions. It can also be seen that the concentration of large particles is significantly lower in the 6-day-old 1-butanol suspension (Fig. 2c) than in the 1-day-old 1-butanol suspension (Fig. 2b). Only particles with maximum radii up to 20 nm were observed in the 6-day-old 1-butanol suspension. A similar situation was observed in the ethanol suspensions. These results indicate a similar final stability of the 1-butanol and the ethanol suspensions. However, a parallel test of concentrated suspensions with an initial concentration of Ba ferrite particles equal to 33 mass% (as opposed to the regular 1 mass%) proved the superior stability of the 1-butanol suspensions over the ethanol ones. Namely, the final saturation concentration of the Ba ferrite particles in the 1-butanol suspensions was significantly higher than in the ethanol: 0.84 and 0.19 vol.%, respectively.

The superior stability of the 1-butanol suspensions was also confirmed with the zeta potential measurements. The zeta potentials of the different suspensions are listed in Table 1. The maximum (absolute value) of the zeta potential in water, −40 mV, was measured at pH $\geq$ 10. However, the zeta potential of these water suspensions at pH $\geq$ 6 was only slightly higher (absolute value) than that of the suspensions of crude Ba ferrite particles (without any addition of the DBSa) [34]. This suggests that the zeta potential of the basic water suspensions originates mainly from the charged particle surfaces and there is no significant interaction between the particles and the DBSa. This is to be expected since the particles' surfaces and the DBSa are both negatively charged at pH > 7. The DBSa, with the chemical formula $HO_3S–C_6H_4–C_{12}H_{25}$, has a polar sulphonic group ($HO_3S–$) and a long, non-polar tail ($–C_{12}H_{25}$) on a benzene ring ($–C_6H_4–$) and dissociates via sulphonic groups ($–SO_3^-$) at pH > 1 (p*K*a < 1). In contrast to this, the 1-butanol suspensions showed a significantly higher and positive zeta potential, 52 mV, which indicates a stronger electrostatic repulsion between the Ba ferrite particles and a higher stability in the 1-butanol than in the water. These suggest that a double DBSa layer was formed around the Ba ferrite particles, as was also confirmed previously with the IR spectroscopy [35]. This is a consequence of the different preparation procedure (see "Suspensions" section) when compared to the water suspensions and can be explained as follows: the positively charged particles' surfaces in acidic water media (pH > 1) enabled the adsorption of the DBSa via the dissociated sulphonic groups onto their surfaces. The DBSa molecules oriented with the polar sulphonic group toward the particles' surfaces, while at the same time the non-polar surfactant tail is oriented into the polar medium (water). This can be written as $P^+—^-O_3S–C_6H_4–C_{12}H_{25}$, where P denotes a particle's surface and — represents a physical bond formed by electrostatic attraction. Such particles are hydrophobic and in acidic water media tend to form flake-like agglomerates. When such particles are washed with acetone, dried and redispersed in 1-butanol the DBSa molecules must rearrange in order to show the positive zeta potential. This can be written, in a very simplified manner, as: $P^+—^-O_3S–C_6H_4–C_{12}H_{25}$ $C_{12}H_{25}–C_6H_4–SO_3^-—H_3O^+$. Due to the same preparation procedure for the ethanol and 1-butanol suspensions, the same stabilization mechanism can be assumed for both of them. The lower value of the zeta potential in ethanol suspensions, 40 mV, when compared to the 1-butanol suspensions, can be attributed to the different polarity of the solvents [35].

## Interaction energy in 1-butanol suspensions

In the following we estimate the conditions for the stabilization of the studied Ba ferrite particles in 1-butanol in order to understand the reason for their stability. We compared the obtained data with the ethanol and water suspensions.

First, we estimated the effect of gravity on the particles with no magnetic field applied. The particle-settling velocity ($v$) due to gravity was calculated using Eq. 8 and compared to the Brownian displacement ($x$) caused by thermal fluctuations that was calculated with Eq. 9 [9].

$$v = \frac{r^2 g(\rho_s - \rho_p)}{18\eta} \tag{8}$$

$$x = \sqrt{\frac{2kTt}{\pi\eta r}} \tag{9}$$

Here, $\rho_s$ is the density of the solvent, $\rho_p$ is the density of the Ba ferrite and $g = 9.8$ m/s$^2$ is the acceleration due to gravity, $T = 293$ K is room temperature, $\eta$ is the viscosity of the solvent and $t = 1$ s time. The materials data are listed in Table 1. The Brownian motion exceeds, by several orders of magnitude, the settling velocity due to gravity, even for the largest particles, suggesting that the gravitational force has no significant influence on the studied particles.

The interaction energy between the particles in the 1-butanol suspensions with respect to their separation distance calculated with Eqs. 1, 2 and 4 is shown in Fig. 3. Note that only the interesting sections of the calculated

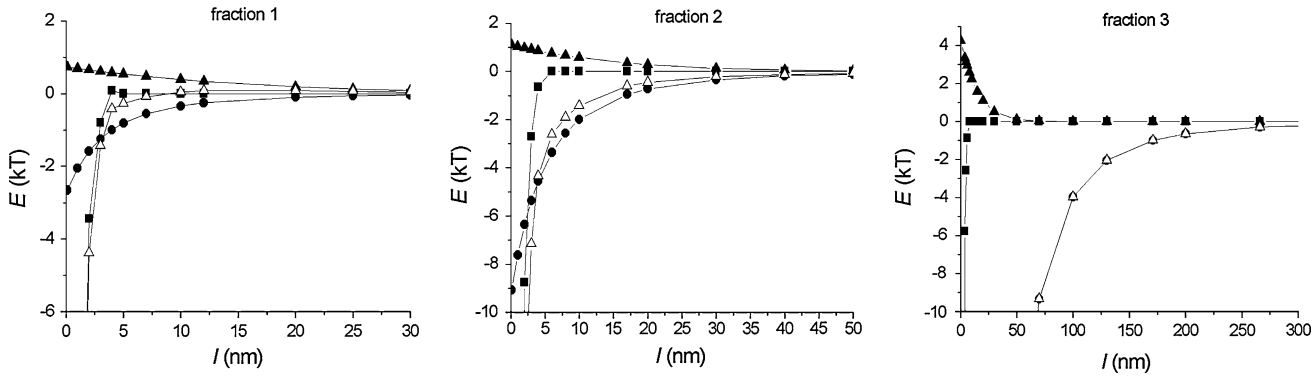


**Fig. 3** Energy of the interaction between the Ba ferrite particles in 1-butanol with respect to the separation distance: van der Waals energy (*squares*), magnetic dipole–dipole energy (*circles*), electrostatic energy (*filled triangles*) and total energy (*empty triangles*)

data are presented, for the sake of clarity, and that the curves of fractions 4 and 5 show no qualitative difference with respect to those of fraction 3. The van der Waals attraction energy between the particles can be neglected with respect to the magnetic dipole–dipole attraction. The absolute values of the attractive interaction energy increase with particle size, while at the same time, the relative contribution of the van der Waals attraction vs. the magnetic attraction decreases. To be precise, the van der Waals attraction energy is only comparable to the magnetic attraction energy at separation distances up to 3 nm for the smallest particles (fraction 1, $r = h = 10$ nm) and this decreases to a separation distance of 1 nm for the largest particles (fraction 5, $r = 65$ nm, $h = 33$ nm).

In general, the magnetic particles will not agglomerate if the thermal energy is larger than the magnetic attraction energy. This also assumes that Brownian motion prevails over the magnetic attraction. The minimum separation distance (Fig. 3; Table 2) at which the thermal energy at room temperature ($4 \times 10^{-21}$ J = 1 kT) exceeds the magnetic attraction energy strongly depends on the particles' sizes, and is between 4 nm for the smallest particles (fraction 1) and 560 nm for the largest particles (fraction 5). This means that the particles should not feel the magnetic attraction when covered with a nonmagnetic layer that has a thickness of 2–280 nm. According to a calculation based on the known bonding lengths and bonding angles in the DBSa molecule, a single layer of DBSa is approximately 2-nm thick. A 100% dense double DBSa layer itself could, theoretically, screen the magnetic attraction between the smallest studied particles, fraction 1. For the larger particles an additional stabilization mechanism should be provided for their stabilization in 1-butanol.

The stabilization of the studied Ba ferrite particles in polar solvents is supposed to be electrosteric: electrostatic due to the dissociation of the sulphonic group (–$SO_3H$) and steric due to the large DBSa molecule ($C_{12}H_{25}$–$C_6H_4$–$SO_3H$). The electrostatic stabilization [9] results from the electrostatic repulsion between the particles and can also be assumed in 1-butanol suspensions of Ba ferrite particles due to their large zeta potential of 52 mV (Table 1). The electrostatic energy, calculated with Eq. 4, is also presented in Fig. 3. The range of the electrostatic repulsion is similar for all the particles' sizes, as was reported before [29]. The maximum electrostatic energy values of the two smallest fractions, 1 and 2, are only around 1 kT, which is small in comparison to the attraction energy, and the total interaction energy ($E_T = E_{vdw} + E_m + E_R$ in Fig. 3) is $\leq$0 kT. Although the repulsive electrostatic energy increases with the particles' sizes, this increase is negligible with the increasing magnetic attraction energy. Therefore, the total interaction energy is in fact equal to the magnetic attraction energy for the large particles, fractions 3–5. It can be concluded that the electrostatic repulsion between Ba ferrite particles with a double DBSa layer is too weak for their dispersion in 1-butanol.

An additional repulsion can be provided, i.e., via steric repulsion. The steric repulsion acts at maximum distances equal to the double thickness of the surfactant layer. Taking into account the maximum possible thickness of the nonmagnetic DBSa double layer ($t = 4$ nm), we can assume that the particles "feel" a steric repulsion at a distance up to 8 nm. Since the magnetic attraction causes the Ba ferrite particles to agglomerate at larger separation distances (Table 2), the steric repulsion has no effect on their stabilization. The only exceptions are the two smallest particle fractions, 1 and 2, with the much weaker and shorter-distance magnetic attraction. To confirm this we estimated their steric repulsion energies (Fig. 4) using Eq. 5 (see Table 1 for the parameter values). The calculated steric energy values increase rapidly with the decreasing separation distance below 8 nm and exceed the attraction energy by two orders of magnitude. The total energy ($E_T = E_{vdw} + E_m + E_R + E_s$ in Fig. 4) shows a high primary maximum for both size fractions. The steric

**Table 2** The separation distance between two Ba ferrite particles ($l^*$) at which the magnetic attraction exceeds the thermal agitation ($|E_m| \geq kT$), the thickness ($t^*$) of the nonmagnetic layer required for screening the magnetic attraction between the Ba ferrite particles, the total interaction energy at distance $l^*$: $E_T' = E_{vdw} + E_m + E_R$ and $E_T'' = E_T' + E_s$; and the total energy ($E_T''$) minimum

| Fraction | $l^*$ (nm) | $t^*$ (nm) | $E_T'$ (kT) | $E_T''$ (kT) | $E_T''$ minimum |
|---|---|---|---|---|---|
| 1 | 4 | 2 | −0.4 | 260 | Not observed |
| 2 | 17 | 8.5 | −0.6 | −0.6 | Secondary minimum −1.9 kT at 8 nm |
| 3 | 171 | 86 | −1.0 | −1.0 | Primary minimum >10 kT at 50 nm |
| 4 | 176 | 88 | −1.0 | −1.0 | |
| 5 | 560 | 280 | −1.0 | −1.0 | |

repulsion significantly exceeds the magnetic attraction of the smallest size fraction 1, even at the 4-nm separation distance (also see Table 2; Fig. 3), at which the magnetic attraction prevails over the thermal agitation in the absence of any repulsion mechanism. Such a distance for the particle-size fraction 2 is at 17 nm, and this is well beyond the steric repulsion range. The total energy at a separation distance of 17 nm is weakly attractive (−0.6 kT) and the secondary minimum of −1.9 kT is observed at a separation distance of 8 nm (see enlargement in Fig. 4). Therefore, the particles from fraction 2 are weakly flocculated and they cannot agglomerate irreversibly due to the large primary maximum resulting from the steric repulsion energy. All these suggest that Ba ferrite particles with $r = h \leq 15$ nm can be dispersed in 1-butanol. In contrast, the magnetic attraction between the particles of larger fractions is too strong and acts over a much longer range. They agglomerate in a primary minimum at distances well beyond the range of the electrosteric repulsion (see also Table 2; Fig. 4).

It was shown previously [36, 37] that providing a strong enough electrostatic repulsive force, which then prevails over the van der Waals attraction between the superparamagnetic particles, results in a secondary minimum under a moderate magnetic field, where particles agglomerate in linear chains. When the magnetic field is turned off, the particles can be spontaneously re-dispersed. However, at a higher magnetic field strength, the particles could not be re-dispersed spontaneously after switching off the field. We can compare the latter case with our results. The large Ba ferrite particles show a strong magnetic interaction (which in fact corresponds to the applied magnetic field in [36]) causing their agglomeration deep into the primary minimum, much deeper than 5 kT. Therefore, such particles, once agglomerated, cannot be re-dispersed again. Only the smallest particles, approaching the superparamagnetic limit [33] and showing the weakest magnetic attraction, can be electrosterically stabilized. This was actually proven experimentally elsewhere [32, 35] using only the particles of the smallest fraction and in this study: the old suspension (Fig. 2c) contained only the particles with $r \leq 20$ nm, which fit roughly into the two smallest fractions. Therefore, we can conclude that the studied Ba ferrite particles cannot be stabilized in 1-butanol with the DBSa unless the large particles are separated and removed.

## Comparison of the stability of the suspensions in different solvents

Finally, we can compare the 1-butanol suspensions with the others, i.e., the water- and ethanol-based suspensions. The calculation of the interaction energy vs. the separation distance only for the smallest particles is shown in Fig. 5 since magnetic attraction completely dominates the interaction energy of the larger particles (Fig. 3). The magnetic interaction energy between the particles is not influenced

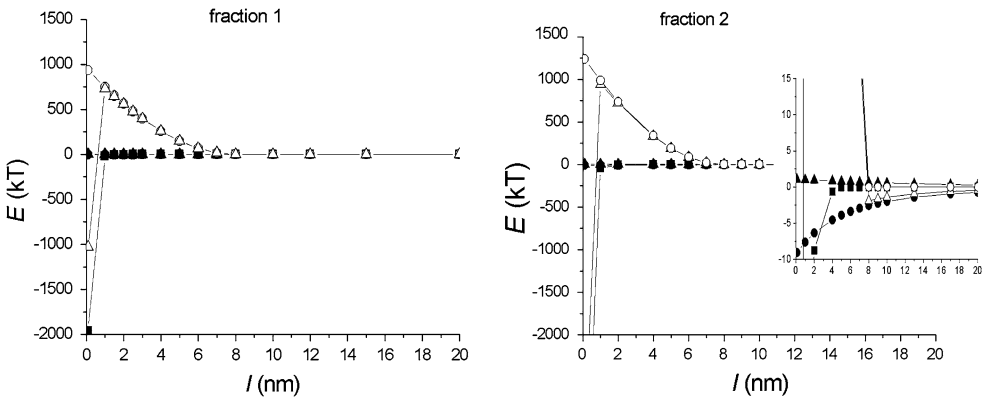


**Fig. 4** Energy of the interaction between the Ba ferrite particles in 1-butanol with respect to the separation distance: van der Waals energy (*squares*), magnetic dipole–dipole energy (*filled circles*), electrostatic energy (*filled triangles*), steric energy (*empty circles*) and total energy (*empty triangles*). *Inset* shows an enlargement around 0 kT for fraction 2

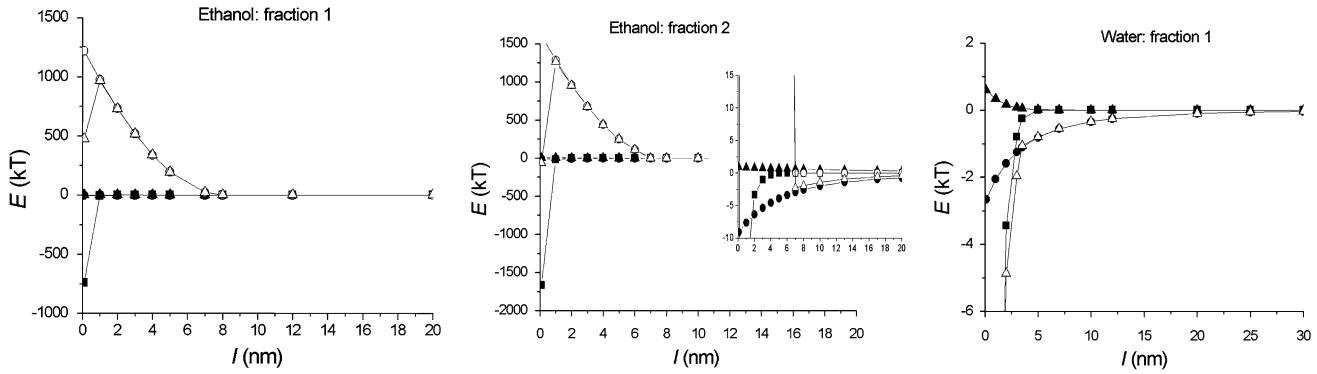


**Fig. 5** Energy of the interaction between the Ba ferrite particles of the smallest fractions in ethanol and water with respect to the separation distance: van der Waals energy (*squares*), magnetic dipole–dipole energy (*circles*), electrostatic energy (*triangles*), steric energy (*empty circles*) and total energy (*empty triangles*). *Inset* shows an enlargement around 0 kT for fraction 2 in ethanol

by the type of solvent. The solvent influences the van der Waals attraction and this influence is determined with the respective Hamaker constant. However, the variation of the Hamaker constant of Ba ferrite in the used solvents is less than an order of magnitude (see "Theory and calculation" section). Therefore, the main difference between the used solvents is the formation of a double layer resulting in a different electrostatic repulsion energy, as was suggested from the significant difference in their zeta potentials (Table 1). The absolute value of the zeta potential in water, 23 mV, was less than half of the value in 1-butanol (52 mV), while ethanol suspensions showed a 39-mV zeta potential. Consequently, the total interaction energy (excluding the steric repulsion) between two particles ($E_T = E_{vdw} + E_m + E_R$ in Fig. 5) is much lower in water than in ethanol and 1-butanol (Fig. 3). We can see no primary maximum for the two interacting Ba ferrite particles (not even for the smallest particles of fraction 1) in water because of the very weak electrostatic repulsion.

As discussed above, only an electrostatic repulsion exists between the Ba ferrite particles in water since no (detectable) amount of DBSa was adsorbed onto their surfaces. The lowest zeta potential and the highest electrolyte ($NH_3$) concentration in the water suspension also result in the lowest electrostatic repulsion energy value, thus explaining their poor stability. In contrast, the interaction behaviour between the two Ba ferrite particles in ethanol is electrosteric ($E_T = E_{vdw} + E_m + E_R + E_s$), similar to that in 1-butanol (Fig. 4). This suggests that the formation of a double DBSa layer was crucial for the stabilization of the smallest particle fractions, 1 and 2.

In general, the strong enough repulsion results in an energy maximum that prevents the agglomeration of the particles if it is large enough (≥5 kT). In the absence of an energy maximum, rapid agglomeration occurs. However, in the presence of an energy maximum, the rate of agglomeration becomes slower. The rate of agglomeration is inversely proportional to the viscosity and the latter increases in the direction of 1-butanol (see Table 1). The calculated rate constants of irreversible agglomeration are listed in Table 3. Equation 7 was only valid for the two smallest fractions of the particles dispersed in 1-butanol or ethanol, while rapid agglomeration, according to Eq. 6, can be expected for all the other fraction/solvent combinations where no primary maximum was observed (Figs. 3, 4, 5). The data in Table 3 show that the main effect on the rate of agglomeration originates from the primary maximum. No particle from the two smallest particles of fraction 1 would agglomerate in 1-butanol or in ethanol. This confirms their stability in 1-butanol and in ethanol. In contrast to this, more than 1000 particles of the same size can agglomerate in 1 s in water. A similar situation is also true for fraction 2. The larger particles (fractions 3–5) agglomerate quickly due to the absence of a primary energy maximum. The rate of rapid agglomeration is the same in a particular solvent,

**Table 3** The rate of irreversible agglomeration of Ba ferrite particles in different solvents: $k_0$ calculated from Eq. 6 and $k$ calculated from Eq. 7 for the fractions 1 and 2 in 1-butanol and ethanol

| Solvent | Fraction | $k_0$ ($k$) ($m^3/s$) | Number of agglomerated particle/s |
|---|---|---|---|
| 1-Butanol | 1 | $\ll 10^{-100}$ | – |
| | 2 | $\ll 10^{-100}$ | – |
| | 3–5 | $1.8 \times 10^{-21}$ | Fractions 3–4 = 22 |
| | | | Fraction 5 = 4 |
| Ethanol | 1 | $\ll 10^{-100}$ | – |
| | 2 | $\ll 10^{-100}$ | – |
| | 3–5 | $4.5 \times 10^{-21}$ | Fractions 3–4 = 55 |
| | | | Fraction 5 = 9 |
| Water | 1–5 | $5.4 \times 10^{-21}$ | Fraction 1 = 1716 |
| | | | Fraction 2 = 509 |
| | | | Fractions 3–4 = 67 |
| | | | Fraction 5 = 12 |

regardless of the particles' sizes. However, the rate of agglomeration in 1-butanol is much slower than in other solvents due to the highest viscosity of 1-butanol. The latter can also be the reason for the experimentally observed superior stability of 1-butanol suspensions over the ethanol suspensions.

To conclude, we showed that it was possible to prepare stabile suspensions in polar solvents from hard-magnetic particles of a limited size and in limited concentrations. This finding is important for the future development of hard-magnetic liquids, since existing ferrofluids are most often prepared from superparamagnetic particles, which possess no remanent magnetization. As an example of the application of Ba ferrite suspensions, the preparation of Ba ferrite thick films with electrophoretic deposition from the studied Ba ferrite suspensions in alcohols was reported in [35].

## Conclusions

We studied the dispersion of hard-magnetic $BaFe_{12}O_{19}$ particles with a broad particle-size distribution (with radii of 10–65 nm and thicknesses of 10–33 nm) in polar solvents. The suspensions with up to 0.8 and 0.2 vol.% of $BaFe_{12}O_{19}$ particles were obtained in 1-butanol and ethanol, respectively. The electrosteric repulsion between the $BaFe_{12}O_{19}$ particles was possible due to the formation of the double DBSa layer in 1-butanol and ethanol, while only a weak electrostatic repulsion due to the particles' surface charge was obtained in basic water suspensions. The calculations of the interparticle interaction energies proved that the small particles, with radii and thicknesses up to 15 nm, could be dispersed in 1-butanol and in ethanol due to a weak magnetic attraction in comparison to the large electrosteric repulsion. The larger particles could not be dispersed under the applied conditions, and for this reason the experimentally obtained suspensions had very low concentrations, below 1 vol.%, of $BaFe_{12}O_{19}$ particles with radii up to 20 nm. Nevertheless, it was shown that stabile, hard-magnetic fluids can be prepared from electrostatically stabilized particles of sufficiently small size.

**Acknowledgements** This work was supported by the Ministry of Higher Education, Science and Technology of the Republic of Slovenia. The authors are grateful to Mr. Stane Čampelj for the zeta potential measurements and to Mr. Sašo Gyergyek and to Mr. Marko Jagodič for the magnetic measurements.

## References

1. Kim JY, Koh JH, Song JS, Grishin A (2004) Phys Status Solidi B 241:1714
2. Erenstein W, Mathur ND, Scott JF (2006) Nature 442:759
3. Sudakar C, Subbana GN, Kutty TRN (2003) J Appl Phys 94:6030
4. Pollert E, Veverka P, Veverka M, Kaman O, Zaveta K, Vasseur S, Epherre R, Goglio G, Duguet E (2009) Prog Solid State Chem 37:1
5. Charles SW (2002) In: Odenbach S (ed) Ferrofluids. Springer, Heidelberg
6. Mueller R, Hiergeist R, Steinmetz H, Ayoub N, Fujisaki M, Eshueppel W (1999) J Magn Magn Mater 201:34
7. Mueller R, Hergt R, Dutz S, Zeisberger M, Gawalek W (2006) J Phys Condens Matter 18:S2527
8. Helgesen G, Skleltorp AT, Mors PM, Botet R, Jullien R (1988) Phys Rev Lett 61:1736
9. Pugh RJ, Bergstrom L (1994) Surface and colloid chemistry in advanced ceramics processing. Marcel Dekker, Inc, New York
10. Rosensweig RE (1997) Ferrohydrodynamics. Dover Publications, Inc., Mineola, New York
11. Tadros Th (1996) Adv Colloid Interface Sci 68:97
12. Bagchi P (1974) J Colloid Interface Sci 47:86
13. Scholten PC (1983) J Magn Magn Mater 39:99
14. Meier DJ (1967) J Phys Chem 71:1861
15. Sheparovich R, Sahoo Y, Motornov M, Wang S, Luo H, Prasad PN, Sokolov I, Minko S (2006) Chem Mater 18:591
16. Makovec D, Košak A, Žnidaršič A, Drofenik M (2004) Nanotechnology 15:S160
17. Batlle X, Garcia del Muro M, Tejada J, Pfeiffer H, Goernet P, Sinn E (1993) J Appl Phys 74:3333
18. de Araujo JH, Cabral FAO, Ginani MF, Soares JM, Machado FLA (2006) J Non Cryst Solids 352:3518
19. Vejpravova J, Plocek J, Niznansky D, Hutlova A, Rehspringer JL, Sechovsky V (2005) IEEE Trans Magn 41:3469
20. Stoia M, Caizer C, Stefanescu M, Barvinschi P, Julean I (2007) J Therm Anal Calorim 88:193
21. Makovec D, Čampelj S, Bele M, Maver U, Zorko M, Drofenik M, Jamnik J, Gabrščček M (2009) Colloid Surf A 334:74
22. Inoue H, Fukke H, Katsumoto M (1990) IEEE Trans Magn 26:75
23. Croucher MD, Milkie TH (1983) Faraday Discuss Chem Soc 76:261
24. Tsouris C, Scott TC (1995) J Colloid Interface Sci 171:319
25. Horn RG, Israelachvili JN (1981) J Chem Phys 75:1400
26. Bergstrom L (1997) Adv Colloid Interface Sci 70:125
27. Tadmor R, Rosensweig RE, Frey J, Klein J (2000) Langmuir 16:9117
28. Roos W (1980) J Am Ceram Soc 63:601
29. Suerig C, Hempel KA, Bonnenberg D (1994) IEEE Trans Magn 30:4092
30. Sankaranarayanan VK, Khan DC (1996) J Magn Magn Mater 153:337
31. Smit J, Wijn HPJ (1959) Ferrites. Philips' Technical Library, Eindhoven
32. Primc D, Makovec D, Lisjak D, Drofenik M (2009) Nanotechnology 20:315605 (9 pp)
33. Kodama RH (1999) J Magn Magn Mater 200:359
34. Lisjak D, Drofenik M (2009) J Appl Phys 105:084908 (8 pp)
35. Ovtar S, Lisjak D, Drofenik M (2009) J Colloid Interface Sci 337:456
36. Chin CJ, Yiacoumi S, Tsouris C (2001) Langmuir 17:6065
37. Ebner AD, Ritter JA, Ploehn HJ (2000) J Colloid Interface Sci 225:39